Effect of Surface Machining on Fatigue of Type 316 Stainless Steel

S. Al-Shahrani, and T.J. Marrow

The University of Manchester, School of Materials, Manchester, UK;

ABSTRACT

The effect of surface finish on fatigue limit of AISI type 316L austenitic stainless steel has been investigated. Fatigue specimens with different surface conditions were obtained by changing the final cutting condition of lathe-turning. The surfaces and near surface microstructures were characterised by electron backscatter diffraction (EBSD), surface profilometry, hardness testing and also X-ray diffraction for residual stress measurement. The fatigue limits were determined in rotating-bending by means of the staircase method. Machined samples were compared with samples that had been electro-polished. Rough machining gave the lowest fatigue limit. Crack nuclei in run-out ($>10^7$ cycles) fatigue tests were observed to arrest at twins, developed by fatigue. The effect of surface roughness is found to be negligible, with a weaker effect of surface residual stress than has been observed for AISI type 304 austenitic stainless steels.

1. INTRODUCTION

The fatigue resistance of austenitic stainless steels can be critical to the performance of pipework and cladding in heat exchangers and cooling systems. Surface machining is used in the fabrication of some of these components, and it is important to be able to assess the likely effects of such surface treatments. This paper reports part of a research program that aims to predict the effects of the surface finish on fatigue in these materials. In previous work three different examples of type 304 stainless steel, with different grain size, were employed in a study of the effect of surface finish on high cycle, stress controlled fatigue. The results indicated insensitivity to surface roughness and sensitivity to the surface residual stress. In this report, a fourth type of austenitic stainless steel (type AISI 316L) has been studied in order to obtain data for one microstructure with different surface finishes. The results are compared with the earlier studies of type AISI 304 steels.

The fatigue specimens were designed using a response surface, which gave an empirical prediction of the effects of machining parameters on roughness and surface residual stress **Error! Reference source not found.**. This had been developed in machining studies of a different microstructure of type 304 stainless steel, and one objective of this work was to test its generality to other austenitic stainless steels. Electron backscatter diffraction (EBSD), surface profilometry, hardness testing and X-ray diffraction stress measurement were employed to characterise the surface and microstructures. The fatigue limits were determined in rotating-bending by means of the staircase method Materials and Experimental procedure

The material used was a type 316L austenitic stainless steel (AISI 316L) supplied in the form of a round bar (dia. 10 mm). The chemical composition is given in Table 1. The grain size was measured (perpendicular to the surface, parallel to the specimen longitudinal axis) from optical micrographs using the linear intercept method. Mechanical properties were obtained using tensile specimens with a gauge diameter of 5 mm, a gauge length of 30 mm at a displacement rate of 2 mm/min.

Table 1: Chemical composition of the type 316L stainless steel (wt %)

Material	***C***	***P***	***S***	***Si***	***Mn***	***Cr***	***Ni***	***Mo***	**Fe**
AISI 316L	0.022	0.042	0.027	0.38	1.57	17.25	10.85	2.07	Bal.

The geometry of the fatigue specimens is given in Figure 1. These were prepared by a numerically controlled lathe.Two different conditions of surface roughness and surface residual stress were produced by changing the final cutting conditions (spindle speed, feed rate and cutting depth). The spindle speed (1500rev. /min) and cut depth (0.4 mm) were the same for both conditions, with a feed rate of 0.25 mm/rev. for the rough machined condition (R) and 0.1 mm/rev. for the fine machined condition (F). The tip radius of the insert tool

was 0.4 mm. These conditions were selected from the response surface to obtain residual stresses that were expected to be either close to zero (fine machined) or tensile (rough machined).

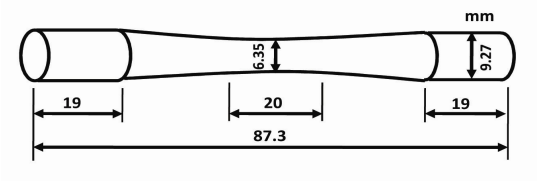

Figure 1: Specimen configuration (circular cross-section).

Surface roughness profiles of machined specimens were characterised using a Taylor-Hobson Talysurf 50 surface Profilometer. The microhardness was measured using an Instron indentation instrument (Wilson model Tukon 2100), with an applied load and load time of 500 g and 10 s, respectively. The residual stress was measured by the $\sin^2\psi$ method using a Proto i-XRD x-ray difractometer. The $\{311\}_{hkl}$ planes were selected at a Bragg reflection of 156^o (2θ) using a Mn-Kα radiation tube with a wavelength λ=0.21nm. The acceleration voltage was 20KV with a current of 4mA. A 1mm collimator was used. Depth profiles of residual stress were obtained using successive electropolishing at intervals of approximately 30µm. The Young's modulus and Poisson's ratio employed were 193GPa and 0.29, respectively. No correction was carried out to account for the material removal of surface layers, as the effect was calculated to be less than 7 %. A set of fatigue specimens was annealed at 900°C for 10 minutesunder an argon gas flow and then electrochemically polished to remove approximately 150 µm from the diameter. Residual stress measurements were obtained from at least two independent specimens for each condition.

The fatigue limits were determined on a R.R Moore rotating-bending machine using the staircase method with sets of 20 specimens, employing a step-width of 2 MPa. The fatigue endurance limit was set at 10^7cycles. Scanning electron microscopy (SEM) and Electron Backscattered Diffraction (EBSD) were used to study the microstructures close to the surface in sectioned metallographic specimens. These were electroplated with Ni to a thickness of approximately 100 µm before sectioning, to improve edge retention. An HKL-EBSD system with a low light CCD camera (Nordlys II), interfaced to a Philips XL-30 FEG-SEM was used for this assessment. Data were acquired using Channel 5 Flamenco HKL software in the beam scanning mode, with an accelerating voltage of 20 kV and a 100 µm aperture. The acquisition time was 60 ms per point, with a step size of 0.5 µm.

2. RESULTS

The grain size of this microstructure was 50µm (standard deviation 5 µm). The measured tensile properties are summarised inTable 2, and are similar to the expected values. The measured surface parameters are given inTable 3. The rough machined surface has significant tensile residual stress (~370 MPa) in comparison to the essentially stress-free fine machined surface (~9 MPa). The expected surface stresses, predicted using the response surface for these machining conditions were 280 MPa and 0 MPa, respectively. Similar surface hardness levels were found for both machining conditions. The lowest hardness was measured on the electropolished samples.

Table 2: Mechanical properties of type 316L (as-received). Two samples tested.

0.2% Proof Stress [MPa]	***Ultimate Tensile Strength [MPa]***
450 & 510	615& 616

The variations of axial residual stress with depth are shown in Figure 2a. Both machining conditions produce a compressive residual stress peak of approximately 300 MPa at a depth of approximately 100 µm. No significant residual stresses were observed beyond approximately 300 µm from the surface. The width of the {311} diffraction peaks (measured as the Full Width at Half Maximum intensity, i.e. FWHM) is shown in Figure 2b. Higher values are obtained within 100 µm of the surface in the machined samples.

The lowest fatigue limit was measured in the rough machined condition, and the highest in the fine machined. The electropolished samples had an intermediate resistance (Table 4). Metallographic observations

of longitudinal sections from run out (10^7 cycles) specimens (The sections were taken perpendicular to the surface, parallel to the specimen longitudinal axis). Figure 3 shows small numbers of crack-like features in all cases.

Table 3: Parameters of machined surfaces (± one standard deviation).

Surface residual stress (MPa)	*Fine Machined*	*8±47*
	Rough Machined	*370±85*
	Electropolished	*-35±21*
Roughness, R_y (µm) (Maximum peak to valley height)	*Fine Machined*	*8±1*
	Rough Machined	*24±1*
Roughness, S (µm) (Average peak spacing)	*Fine Machined*	*30±2*
	Rough Machined	*94±23*
Surface Microhardness, Hv	*Fine Machined*	*332±3*
	Rough Machined	*315±3*
	Electropolished	*208±2*

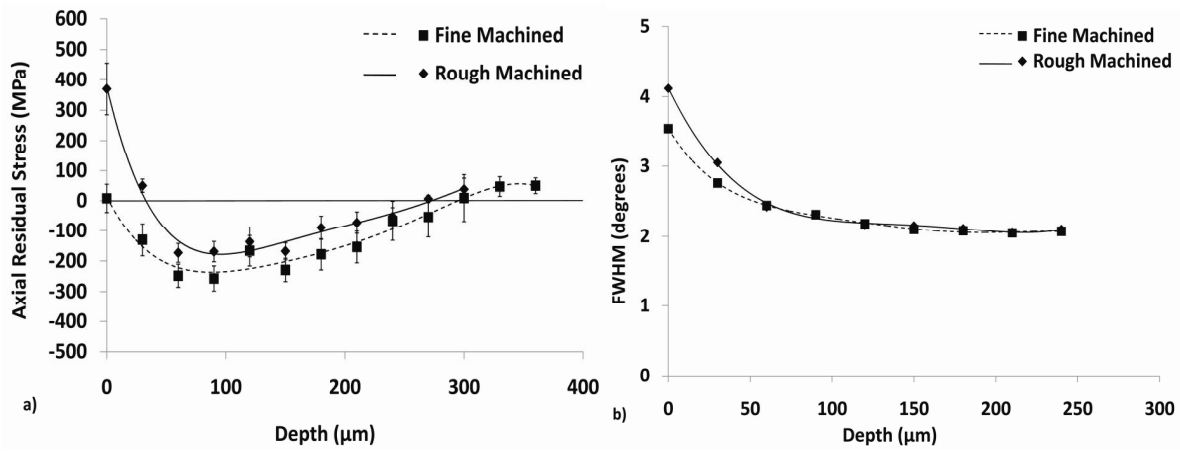

Figure 2: a) Variation of axial residual stress with depth for machined surfaces. Approximate trend lines added for visualisation, b) Variation of {311} diffraction peak width (FWHM) with depth for machined surfaces.

The Kikuchi "band contrast" mapsobtained by EBSD are sensitive to plastic strain and can be used to reveal slip bands. Significant plastic deformation was observed near the surface of samples that has been fatigued (e.g. Figure 4a and b). This behaviour was observed for all fatigued specimens of each condition. Cracks can be seen in Figure 4a in a typical run-out of Electropolished specimen at 306 MPa. The pole figure for the {111} planes obtained from the lamellar features (T) and matrix (M) is shown in Figure 4d.

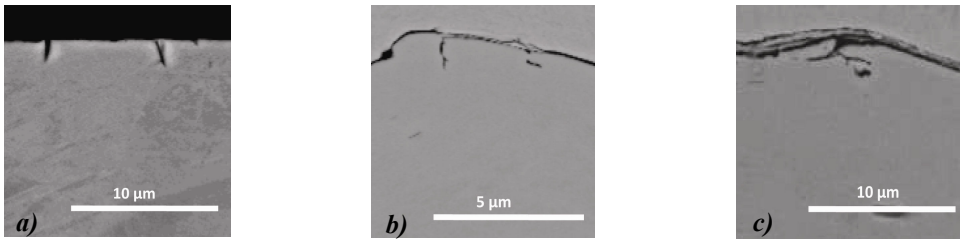

Figure 3: Crack-like features in fatigued (run-out) specimens: a) Electropolished, b)Rough machined, c) Fine machined.

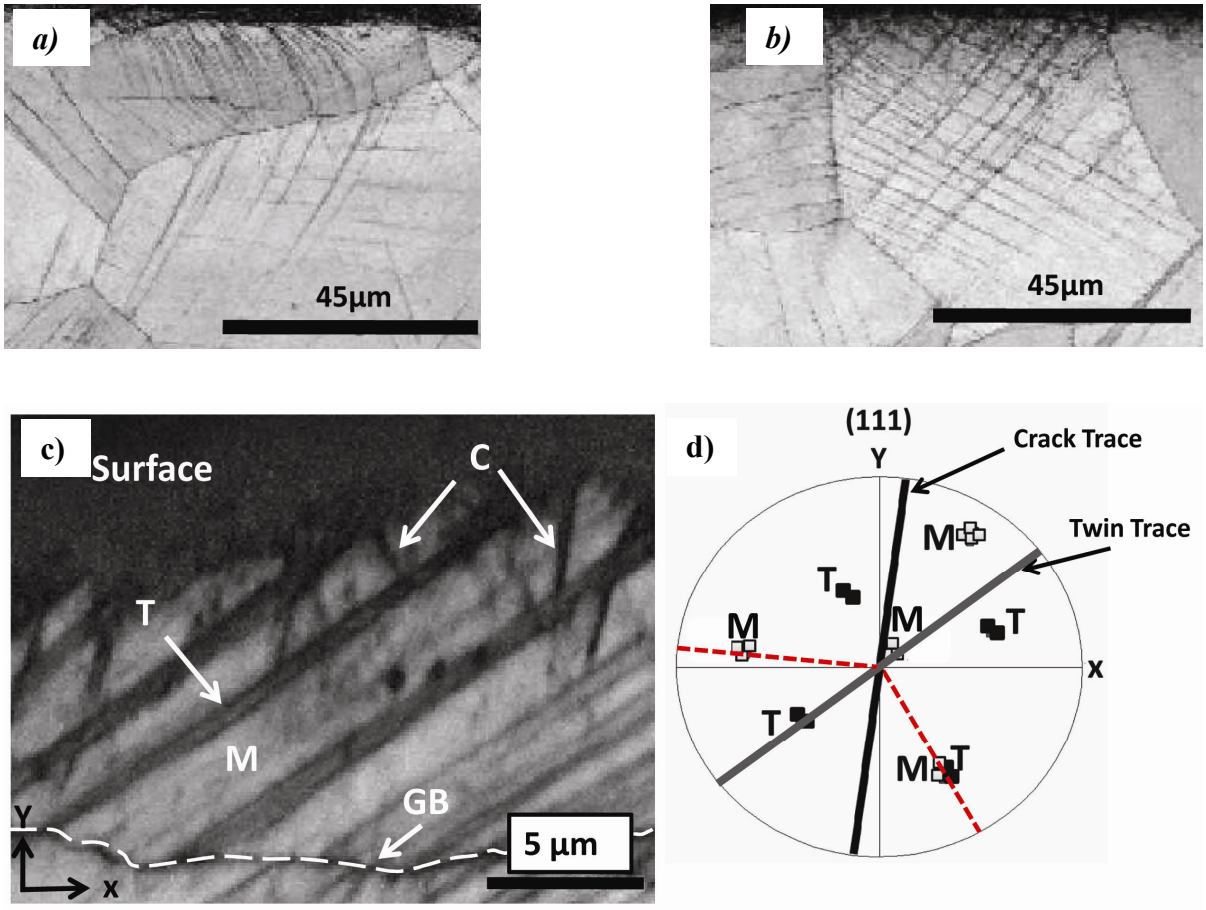

Figure 4: a) Fine machined specimen fatigued at 304 MPa, b) Electropolished specimenfatigued at 306 MPa, c) Arrested cracks by twins [C: Crack, T:Lamellar Features, GB: Grain Boundary, M: Matrix] in fatigued specimen (Electropolished specimen fatigued at 306 MPa),d) {111} pole figure shows the orientations of the lamellar features and matrix in c).

Table 4: Fatigue limits obtained by staircase method (± one standard deviation) (~20 samples tested in each condition).

Condition	**Fatigue Limit (MPa)**
Fine Machined	*318±3*
Electropolished	*302±5*
Rough Machined	*291±2*

3. DISCUSSION

The surface residual stresses of 8 ± 47 MPa and 370 ± 85 MPa are in fair agreement with the stresses of 0 MPa and 280 MPa predicted by the response surface. The measured surface and microstructure parameters (Table 3) were used to calculate the fatigue crack propagation threshold stress for each condition, using an implementation of the Navarro-Rios (N-R) short fatigue crack model. The methodology is described in detail in reference. An important parameter in the model is the characteristic distance between the microstructural barriers that are assumed to resist crack propagation. The N-R short crack model is most sensitive to stress gradients that act over a similar length scale to the barrier spacing. This is commonly taken to be the grain size. The compressive subsurface residual stress peak from machining is thus predicted to have a significant effect on crack propagation, as is the stress concentration from the surface roughness **Error! Reference source not found.**. The fatigue limit is the minimum stress amplitude required for unstable propagation of a crack nucleus (Figure 5a). Using the grain size as the barrier spacing leads theN-R model to predict significant differences in the fatigue limit between the machining conditions; but this does not agree with the experimental observations (Figure 5b). This discrepancy in type 316 stainless steels is consistent with previous observations in type 304

austenitic stainless steels The electropolished samples clearly show stable fatigue crack nuclei (Figure 3a). However, the irregular surface features observed in the rough machined samples are associated with defects introduced by machining. These would be more significant stress raisers than the surface roughness, and are assumed to act as potential fatigue crack nuclei. All run-out fatigue samples therefore show stable defects with a depthof a few μm.

In Figure 4c, it is clear that the short cracks in an electropolished run-out specimen are arrested at the boundaries of lamellar features. Their misorientation and habit plane (indicated by their trace) is that of coherent twins **Error! Reference source not found.**. This shows that twins may act as barriers to fatigue crack nuclei. The crack traces are also close to those of {111} planes, indicating have stage I crystallographic character. The misorientation between the matrix and twins would present a significant barrier to this shear mode of fatigue crack propagation. For such barrier spacing, using the N-R model, the fatigue behaviour can be expected to be insensitive to the longer-range sub-surface compressive residual stress peak and sensitive to the residual stress conditions closest to the surface.

The effect of surface residual stress on the fatigue limit of three type 304 austenitic stainless steels with different grain size, is shown in **Error! Reference source not found.**a. The hardness of these alloys in the electropolished and annealed conditions differ, and this has a significant effect in their relative fatigue limits. The same data are shown in b as the change in fatigue limit relative to the electropolished (annealed) condition. This shows sensitivity to surface residual stress for the type 304 steels. However, the fatigue limit of the type 316 shows much less sensitivity to the surface stress.

The deformation characteristics of the two alloy types differ. For example, the surfaces of fatigued type 304 stainless steels develop martensite **Error! Reference source not found.**, which does not occur in the more stable type 316 stainless steels. Work is in progress to identify the microstructural barriers and mode of crack propagation (i.e. stage I or stage II) in type 304 steels in order to understand their relative sensitivity to surface finishing.

4. CONCLUSION

Rough machining on a lathe, using a high feed rate, introduced significant tensile residual stress at the machined surface of a type 316L austenitic stainless steel, whereas fine machining gave a negligible stress. Both rough and fine machining cause significant sub-surface compressive residual stresses. Rough machining gave the lowest fatigue limit. Crack nuclei in run-out ($>10^7$ cycles) fatigue tests were observed to arrest at twins, developed by fatigue. The effect of surface roughness is found to be negligible, with a weaker effect of surface residual stress than has been observed for AISI type 304 austenitic stainless steels. This is explained by a significant interaction between the crack nuclei and the cyclic plastically deformed microstructure, which limits the stable crack nucleus size to the near surface region.

Acknowledgements

The authors would like to thank Saudi Basic Industries Corporation (SABIC) for financial support of S-A.

5. REFERENCES

[1] S. Al-Shahrani, T.J. Marrow, Effect of surface finish on fatigue of stainless steels, 12th International Conference of Fracture,ICF12, Ottawa, (July 2009) CANADA.
[2] M. Kuroda, T.J. Marrow, Modeling the effects of surface finish on fatigue limit in austenitic stainless steels, Fatigue FractEngng Mater Struct(2007)**31**,1-18.
[3] M. Kuroda, T.J. Marrow, Analyses of the effects of surface finish on fatigue limit in austenitic stainless steels by mechanistic modeling, 9th International Fatigue Congress, Atlanta, (2006) USA.
[4] M. Kuroda, T.J. Marrow and A.H. Sherry, Effects of surface finish on fatigue in austenitic stainless steels, 16th European Conference on Fracture, ECF16, Alexandropoulis, Greece, (2006), Ed. E.E. Gdoutos.
[5] BRITISH STANDARD, Methods of Fatigue Testing —Part 5: Guide to the application of statistics, BS 3518-5:1966.
[6] M. Kuroda, T.J. Marrow, Preparation of Fatigue specimens With Controled Surface Characteristics, Journal of Materials ProcessingTech. (2008)**203**, 396-403.

[7] M.G. Moore, W.P. Evans, Mathematical correction for stress in removed layers in X-ray diffraction residual stress analysis, SAE Trans, (1958) **66**,340-345.
[8] R. M'Saoubi, L. Ryde, Application of the EBSD technique for the characterisation ofdeformation zones in metal cutting, Materials Science and Engineering A (2005) **405**,339–349.
[9] A. Yamamoto, T. Yamada, Effects of Surface Grinding on Hardness Distribution and Residual Stress in Low Carbon Austenitic Stainless Steel SUS316L, ISIJ International (2004)**44**,1780–1782.
[10] J.P. Lucas, and W.Gerberich, Proposed criterion for fatigue threshold: dislocation substructure Fatigue of Engineering Materials and Structures (1983)**6**, 271-280.
[11] Robert E., Reed-Hill, R. Abbaschian, Physical Metallurgy Principles, Third Edition.
[12] Vallellano, C., Mariscal, M. R., Navarro, A micromechanical approach to fatigue in small notches. Fatigue Fract. Engng Mater. Struct. (2005)**28**, 1035-1045.
[13] Vallellano, C., Navarro, A. and Dominguez, J., Fatigue crack growth threshold conditions at notches part I: theory. Fatigue Fract. Engng Mater Struct,(2000)**23**, 113-121.

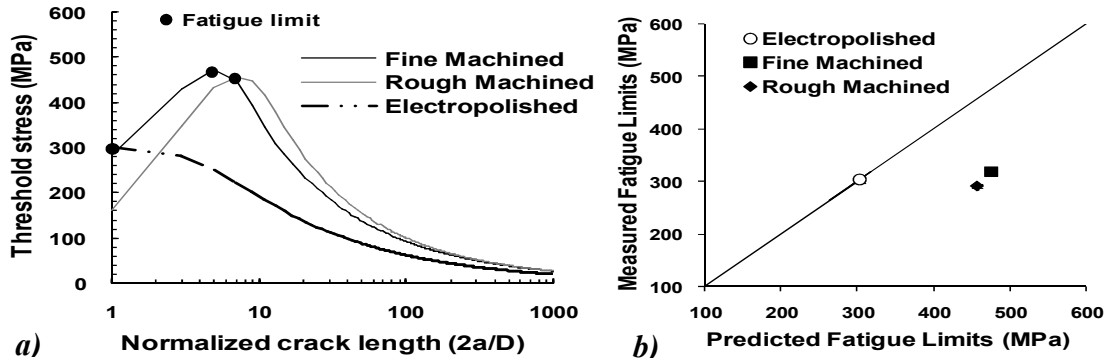

Figure 5: a) Threshold stress profiles predicted for; as machined specimens, annealed specimens and electropolished specimens, b) Predicted fatigue limit in comparison with the measured fatigue limit (N-R Model). (Crack length, a*, and grain size,* D*).*

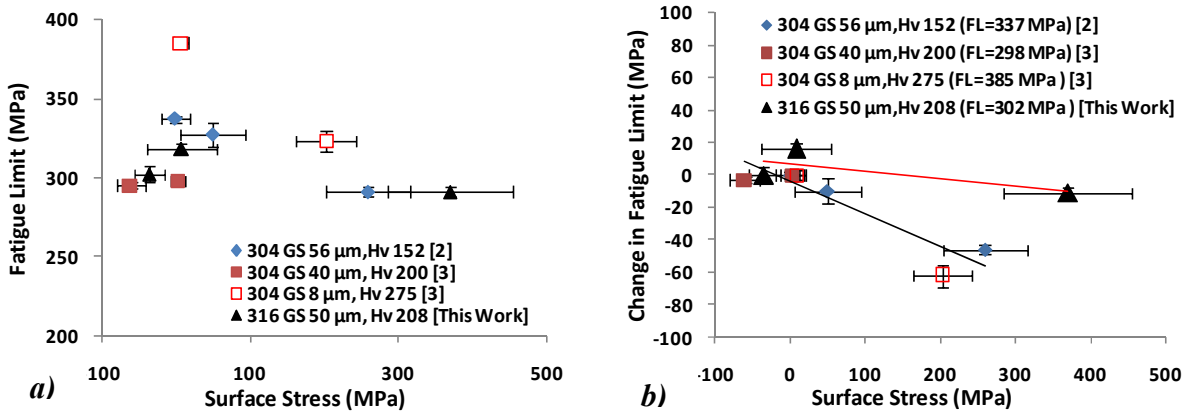

Figure 6: The effect of surface residual stress on the fatigue limit, a) measured fatigue limit b) change in fatigue limit relative to the intrinsic fatigue limit for electropolished samples (Gs: Grain Size; Hv: Hardness; FL: Fatigue Limit of electropolished and annealed).